DR MOHAMMAD K. HAJIHOSSEINI (Orcid ID : 0000-0001-7960-5114)

Article type : Original Article

Characterization of endogenous players in Fibroblast Growth Factor-regulated functions of hypothalamic tanycytes and energy-balance nuclei

Benediktas Kaminskas[1], Timothy Goodman[1], Andrew Hagan[2], Saverio Bellusci[3,4], David M. Ornitz[2] and Mohammad K. Hajihosseini[1,4*]

[1]School of Biological Sciences, University of East Anglia, Norwich, NR4 7TJ, UK

[2]Department of Developmental Biology, Washington University School of Medicine, St. Louis, Missouri, USA

[3]Cardio-Pulmonary Institute, Justus Liebig University, 35392, Giessen, Germany, [4]International Collaborative Centre on Growth factor research, Life Science Institute, Wenzhou Medical University, Wenzhou, Zhejiang Province, China

* Author for correspondence: email m.k.h@uea.ac.uk

Acknowledgements

We are grateful to Stuart Nayar for insightful comments and critique. BK was supported by a BBSRC Doctoral Training Programme (DTP) Studentship allocated to MKH. This works was supported in part by a BBSRC research grant (BB/L003406/1) to MKH. SB was supported by EXC2026 (project id 390649896). The authors apologies to colleagues whose work could not be cited due to space limitations.

Data Availability Statement

The data that support the findings of this study are available from the corresponding author upon reasonable request.

This article has been accepted for publication and undergone full peer review but has not been through the copyediting, typesetting, pagination and proofreading process, which may lead to differences between this version and the Version of Record. Please cite this article as doi: 10.1111/jne.12750

Running title: Fibroblast growth factors in postnatal tanycytes and mediobasal hypothalamic nuclei

Key words: FGF functions in hypothalamus; tanycytes: gene expression.

28 pages: 5 Figures, 1 Table, 2 Supplementary Tables and 3 Supplementary Figures.

Abstract

The mammalian hypothalamus regulates key homeostatic and neuroendocrine functions ranging from circadian rhythm and energy-balance to growth and reproductive cycles via the hypothalamo-pituitary and hypothalamo-thyroid axes. In addition to its neurons, tanycytes are taking centre stage in the short and long term augmentation and integration of diverse hypothalamic functions, but the genetic regulators and mediators of their involvement are poorly understood. Exogenous interventions have implicated Fibroblast growth factor (FGF) signalling, but the focal point of FGF action and any role for putative endogenous players also remains elusive. We carried out a comprehensive high-resolution screen of FGF signalling pathway mediators and modifiers using a combination of *in situ* hybridization, immunolabelling and transgenic reporter mice, to map their spatial distribution in the adult hypothalamus. Our findings suggest that beta tanycytes are the likely focal point of exogenous and endogenous FGF action in the third ventricular wall, utilising FGF-receptors (FGFRs) -1 and -2 IIIc isoforms, but not FGFR3. Key IIIc-activating endogenous ligands include FGFs 1, 2, 9 and 18, which are expressed by a subset of ependymal and parenchymal cells. In the parenchymal compartment, FGFRs 1-3 show divergent patterns, with FGFR1 predominant in neuronal nuclei and FGFR3 expression being associated with glial cell function. Intracrine FGFs are also present, suggestive of multiple modes of FGF function. Our findings provide a testable framework for understanding the complex role of FGFs in regulating the metabolic endocrine and neurogenic functions of hypothalamus in vivo.

Introduction

Growing evidence shows that in addition to hypothalamic neurons, tanycytes act as sensors, mediators and effectors for critical processes that underpin the homeostatic and neuroendocrine functions of hypothalamus, for example, sensing of metabolites and micronutrients and trafficking of peripheral and central signals such as Leptin and Gonadotropin-releasing hormone (GnRH) (1, 2). Moreover, a subset of tanycytes acts as bona fide neural stem/progenitor cells (NSPCs) in the postnatal and adult hypothalamus, capable of generating new energy balance-regulating neurons, and glia (3-5). Tanycytes are residual radial glial-like cells that occupy the floor and ventro-lateral walls of the third ventricle (3V). They have been subdivided into four main subtypes: Beta (β) 2, 1 and alpha (α) 2 and 1, according to a combination of projection trajectory, morphology, barrier properties, cilia arrangement and positioning within or outside marker domains within the 3V wall (1). Commonly, their apical surface is exposed to the cerebrospinal fluid (CSF) whilst their basal processes either contact the portal capillaries of the central (β2-tanycytes) and lateral (β1-tanycytes) median eminence, or terminate within the arcuate or ventromedial and dorsomedial nuclei (α-tanycytes), whose neurons are crucial for maintaining energy homeostasis and related food-seeking behaviour.

Fibroblast growth factors (FGFs) are emerging as important regulators of tanycyte biology and hypothalamic neuronal function. The mammalian FGFs number 22 in total, 18 of which function as paracrine, endocrine or autocrine molecules by activating one of four types of FGF receptors (FGFRs 1-4) and the ensuing downstream intracellular signalling pathways: Ras-Raf-MAPK, PI3K-AKT and PLCγ (6, 7). The remaining FGFs (11-14) function intracellularly in a receptor-independent manner (8). FGFR signalling can modulate diverse aspects of cell behaviour in a cell-type specific manner. This is achieved partly through differential levels of signalling, established by intracellular negative feedback loop regulators such as Sproutys (Spry) and Map-kinase phosphatases (Mkp)(9). Tissue specificity of FGF action is governed by target cells' expression of the so-called IIIb or IIIc alternatively-spliced receptor isoforms which engage a mutually-exclusive set of FGFs (10). Moreover, co-factors such as sulphated proteoglycans (SPGs) and β□Klotho molecules not only facilitate focal FGF/FGFR signalling but also determine the range of extracellular FGF diffusion. For example, peripherally generated FGFs -19 and -21

evade entrapment by Heparan Sulphate Proteoglycans (HSPG) to act as circulating hormones in the metabolic control of energy homeostasis, with potential clinical applications in the management of type 2 diabetes (11, 12).

Exogenous FGF2 is a potent mitogen for hypothalamic ependymal and neural cells *in vitro* and *in vivo* (5, 13). Levels of FGF1 show a dramatic postprandial rise in the cerebrospinal fluid (CSF) (14, 15), whilst experimental elevation or attenuation of canonical FGF signalling, via peripheral or intracerebroventricular (ICV) application of FGF ligands, soluble FGFR fragments or neutralizing antibodies, can respectively induce hypo- and hyperphagia (16-19). Exogenous FGF1 also accelerates glucose clearance and induces sustained remission of diabetes symptoms in a diabetic mouse model (20).

A full understanding of how exogenous FGFs function and/or whether endogenous FGFs have similar or unique roles, requires the identification and spatial distribution of the key players – ligands, receptors, receptor co-factors and signalling modifiers. To address this need, we carried out a detailed survey of FGF signalling pathway components in mediobasal hypothalamus, using RT-PCR screens, in conjunction with *in situ* hybridization, immunolabelling and analysis of transgenic reporter mice. Our investigations reveal intricate and restricted domains of FGF and FGFR receptor expression amongst tanycytes, in addition to distinct as well as overlapping patterns of receptor and ligand expression within the neighbouring energy balance regulating nuclei.

Materials and Methods

Animals

Both male and female mice ranging in age from 30 to 80 days of age were used. All mice were bred and maintained on a mixed C57BL6/129Ola background, under a 12-hour light/dark cycle, in accordance with local and national regulations and licenses governing experimental work with animals. Tissues from *Fgf9-LacZ*; *Fgf18*-CreER and *Etv4*-GFP transgenic reporter mice were kindly provided by Professors David Ornitz and Saverio Bellusci, from previously described (21, 22) or recently generated strains. To detect Fgf18 expressing cells in the brain, mice carrying *Fgf18*-

CreER::Rosa-tdTomato alleles were injected intraperitoneally with tamoxifen (300 mg/ kg body weight) at P50, P51 and P52, before tissue harvest at P53.

Tissue isolation and preparation

Mice were culled by CO_2 asphyxiation and brains were then dissected out and fixed for 4-16 hours overnight in 4% paraformaldehyde (PFA, pH 7.0) at 4°C. For fresh tissue and mRNA isolation, mice were culled by cervical dislocation and micro-dissected hypothalami were flash frozen in cryotubes on dry ice and stored at -80 °C. To generate cryostat sections, the brains were washed with DEPC-treated PBS (DEPC-PBS) and cryo-protected in 30% w/v sucrose /DEPC-PBS solution for 48 hours at 4 °C. Thereafter, they were placed in cryomoulds filled with optimal cutting temperature (OCT) compound, allowed to set on dry ice, and stored at -80 °C. 20 µm thick coronal sections containing the central part of median eminence (Bregma -1.45 to -1.94) were then generated using a freezing microtome (MicroM HM560) and thaw-mounted onto previously baked (180°C, overnight) Superfrost (ThermoFisher Scientific) slides, and stored at -80 °C until use.

To generate vibratome sections, PFA-fixed brains were first dehydrated in ascending concentrations (30%, 50%, 70%, 90%; 1 hour per dilution) of ethanol, before being stored at 4 °C in absolute ethanol. Just before use, brains were rehydrated stepwise back to PBS and embedded in 3% w/v agar overnight. Coronal 60 µm-thick sections containing median eminence (Bregma -1.46 to -2.18) were then generated using a vibrating microtome (Leica), and stored in PBS until use.

RNA isolation

Microdissected hypothalami were homogenised by trituration in 1 ml of TRIzol (Invitrogen) before addition of 200 µl of chloroform. Following centrifugation (15 minutes at 12,000 x*g)*, RNA was precipitated from the aqueous layer by addition of 500 µl of Isopropanol. Samples were briefly vortexed, allowed to stand for 10 minute at RT and then centrifuged (15 minutes at 12,000 xg). The resulting supernatant was

carefully removed before adding 1 ml of 75% ethanol diluted in molecular grade water (Sigma) and further centrifugation (12 minutes at 5,200 xg). The RNA pellet was then briefly air dried, re-suspended in molecular grade water and incubated at 55 C° for 10 minutes. RNA concentration and quality was determined using a spectrophotometer (Nanodrop ND-1000, Thermo Scientific) and samples were stored at -80 C° until use.

Primer design and Reverse-Transcriptase PCR

Gene specific primer pairs (Supplementary Table 1) for use in RT-PCR reactions were designed using NCBI primer-BLAST, aiming for regions of least sequence conservation between related family members (23), and amplicons that are not only small but are also comparable in size across the related family members (Suppl. Table 1). To rapidly generate gene-specific templates for *in vitro* transcription of antisense cRNA probes (see below), some reverse primers were additionally tagged at their 5' end with a T7 polymerase-encoding promoter sequence (TAATACGACTCACTATAGGG) (23). RT-PCR reactions were carried out in a thermocycler (MJ ReseArch) using *illustra Ready-To-Go™* RT-PCR beads (GE Healthcare Life Sciences) and 1μg of hypothalamic RNA per reaction. For first strand synthesis, Oligo $(dT)_{12-18}$ primers (Invitrogen) and the following cycles were used: 15 min at 42 °C; 5 min at 95 °C; and 15 min at 6 °C. After addition of 1.5 pmol of forward and reverse gene-specific primers, PCR was carried out using: 30 sec at 95 °C, then 34 cycles of 30 s at 60 °C; 1min at 68 °C; followed by 15 mins at 6 °C. The products were resolved alongside 1Kb DNA ladder on 1% w/v agarose gel and visualised using ethidium bromide. RT-PCR reactions with β-Actin primers served as positive control.

Riboprobe synthesis and *In situ* hybridization

Digoxigenin-labelled antisense RNA probes were generated using T7 RNA polymerase enzyme (ThermoFisher Scientific) and either T7-tagged RT-PCR amplicons (above) or linearized plasmids encoding gene-specific cDNAs

(Supplemental Table 2), as templates. Riboprobes were purified using Chroma Spin columns (Clontech) and stored at -20 °C until use.

In situ hybridization (ISH) reactions were performed after optimization of published protocols (24) as detailed below. Briefly, cryosections were allowed to equilibrate at room temperature for 1 hour before a 5 minute fixation in 4% PFA followed by three 5 min washes with DEPC-PBS. Sections were then treated for 50 mins with 1µg/ml proteinase K in a buffer of 50 mM pH 8.0 Tris-HCl, 5 mM EDTA, and post-fixed with 4% PFA for 5 minutes. After three 5 minute washes with DEPC-PBS, sections were incubated for 10min in acetylation solution (1.4% triethanolamine, 0.2% HCl, 0.25% acetic anhydride). Prehybridization was carried out for 4 hours in hybridization buffer (50% formamide, 5x salt sodium citrate buffer (SSC), pH 7.0, 5x Denhardt's solution, 0.25 mg/ml salmon sperm DNA, 0.5 mg/ml yeast tRNA). Hybridization was carried out at between 68-72 °C in a hybridization oven for 16-18 hours, using 500 ng/ml of riboprobes diluted in hybridization buffer. Post hybridization washes were: 5 mins with 5x SSC at RT, followed by three 30 min washes with 0.2x SSC at hybridization temperature and a wash with 0.2x SSC at RT. Sections were then washed with Tris-HCl/saline buffer (100 mM Tris-HCl, pH 7.5, 150 mM NaCl) at RT and blocked in Tris-HCl/saline buffer with 10% heat-inactivated Normal Goat Serum (hiNGS) before an overnight incubation at 4 °C with alkaline phosphatase-conjugated anti-digoxigenin conjugated antibodies (Supplementary Table 2) diluted in Tris-HCl/saline buffer, containing 3% hiNGS. Excess primary antibody was removed by six 15 min washes in Tris-HCl/saline buffer. Colour reaction was carried out in NTM buffer (0.1 M Tris-HCl, pH 9.5, 0.1 M NaCl, 50 mM $MgCl_2$) containing 2 mM Levamisole, 375 µg/ml NBT and 187.5 µg/ml BCIP, and allowed to progress at 4 °C until a signal became visible. The reactions were stopped by three 5 min washes with PBS, followed by a 1-hour wash in 95% ethanol. Sections were then rehydrated for 15 mins in d.d. H_2O before being coverslipped in 50%/PBS glycerol.

Negative controls included the omission of antisense and/or use of sense cRNA probes (*Fgf9, Fgf20, Klb, Sef, Spry1, Spry2*). Positive controls included probes for Neuropeptide Y (Npy), an anorexigenic neurotransmitter expressed by some arcuate neurons, which invariably yielded a very strong and specific signal.

Immunohistochemistry, immmuno-fluorescent labelling and X-gal staining

Nonspecific binding sites were blocked by a 2 hour incubation in a solution of 20% hiNGS/ 1% Triton X-100 (TX)/PBS, before application of primary antibodies (Supplementary Table 2) overnight at 4 °C in 0.2% hiNGS/ 0.1% TX/PBS. Excess primary antibodies were removed by five 1 hour washes at RT with a 0.2% hiNGS/ 0.1% TX solution and this was followed by overnight incubation with the relevant secondary fluorophore conjugated antibodies (Supplementary Table 2) diluted in 0.2% hiNGS/ 0.5% NP-40/ in PBS at 4 °C. The next day, sections were washed six times (30 min per wash) before counterstaining with nuclear DNA marker, Hoechst, and subsequent mounting in Vectashield (Vector Labs).

For combined ISH and Immunohistochemistry, after completion of the ISH protocol, sections were incubated for 1 hour in blocking solution (10% hiNGS/0.3% TX/PBS) followed by overnight incubation at 4 °C with mouse anti-GFAP, rabbit anti-GFAP or mouse anti-S100β antibodies (Suppl. Table 2) diluted in 0.2% hiNGS/ 0.1% TX/ PBS. After three 5 min PBS washes, the DAB staining reaction was performed using a DAB peroxidase substrate kit (Vector Labs) according to the manufacturer's instructions. After five 1 min washes with double distilled water, sections were preserved by coverslipping with 50% glycerol/PBS solution.

To detect the product of the lacZ-reporter gene, β-galactosidase, brains of Fgf10-lacZ reporter mice were preserved in Mirsky's fixative (National Diagnostics) overnight at 4 ºC, washed three times with PBT (PBS with 0.1% Tween-20) before being incubated with the X-gal substrate solution (2 mM $MgCl_2$, 5 mM $K_4Fe(CN)_6.3H_2O$, 0.02% v/v NP-40, 0.1% v/v X-Gal; diluted in PBS) at 37 ºC for 30 minutes. Samples were then post fixed with 4% PFA, and dehydrated into absolute ethanol for subsequent use and sectioning (see above).

Image capture and analysis

All images were captured using a Zeiss Axioplan 2 microscope and Axiovision 4.8 software. High magnification of pERK immunostaining was imaged and analysed by 3D reconstruction of 1 µm optical sections (z stacks), captured using an Apotome attachment. Images were post-processed (adjustment of brightness, contrast, levels and unsharp mask) using FIJI, Axiovision and Photoshop software packages.

Results

Global analysis: detection of distinct FGFs and signalling modulators and predominance of FGF-receptor IIIc isoforms

To determine which components of the FGF signalling system need to be mapped spatially in the hypothalamus, we first undertook a gross RT-PCR screen of mRNA expression derived from 30 to 45 day-old (P30-P45) animals. Industrially pre-aliquoted substrates (illustra Ready-To-Go beads) were used to amplify comparable amplicon sizes. We opted for an RNA-based and gene-reporter analysis (here and below) as antibodies to FGFs often detect multiple related family members, and in the case of FGFRs, fail to discriminate between isoforms in immunolabellig studies. Animals older than P30 were used as the full spectrum of tanycytes subtypes as well as the connectivity of hypothalamic neurons is fully established by this age (25).

FGFRs 1 to 3 exist as alternatively-spliced isoforms termed 'IIIb' and 'IIIc', depending on alternate usage of exons that encode the amino half of the receptors' third extracellular Ig-like domain, whereas FGFR4 possesses only the IIIc form. Use of isoform-specific primers showed that FGFRs 1-3 are the predominantly expressed receptors, specifically, their IIIc isoforms (Fig. 1A), suggesting that IIIc-activating FGF ligands are the likely drivers of canonical FGFR signalling in hypothalamus.

Use of primer pairs for all 22 mouse *Fgfs* (Supplementary Table1) detected products of the expected size for *Fgf*s *-1, -2, -5, -7, -8, -9, -10, -11, -12, -13, -14, -16, -17, -18, 20* and *21* (Fig. 1B,B'). Multiple bands were detected for *Fgfs* -5 and -8, possibly representing their closely related isoforms (26). Co-receptor Klotho-β, which is required for FGF-19 and -s21 action, as well as FGFR signalling modulators *Spry1*,

Spry2, *Spry3* and *Mkp3* but not *Sef* or *Spry4*, were also detectable, with *Sprys* -2 and -3 showing stronger expression (Fig. 1C). *Pea3* (also known as *Etv4*), a transcriptional target of FGF signalling was also present.

This broad screen reveals that various components of the FGF signalling pathway are in place to mediate exogenous and to potentially augment endogenous FGF signalling in the hypothalamus.

Predominance of Fgf receptors -1 and -2 in β-tanycyte domain

The gross RT-PCR screen (above) was performed using bulk tissue that contains multiple cell compartments – the Median Eminence (M.E.), the ependymal cell wall and the hypothalamic parenchyma. To delineate specific expression of FGF signalling apparatus in tanycytes and the flanking mediobasal nuclei - Arcuate (Arc), ventromedial (VMN), dorsomedial (DMN) and lateral hypothalamus area (LHA) - at high resolution, we performed mRNA *in situ* hybridization on coronal sections containing the central part of the M.E. (Bregma -1.45 to -1.94) from P60-P80 mice. Because the expression of astroglial marker, GFAP, is normally prominent in the α-tanycyte domain and dorsal ependymal cells, and absent from β-tanycyte domain (1, 4)(Suppl. Fig. 1), the in situ hybridization analysis was combined with mouse anti-GFAP immunolabelling to investigate the selective expression of candidate genes within alpha vs beta tanycyte subtypes.

We found that *Fgfr1* and *Fgfr2* are expressed predominantly in the GFAP-ve β-tanycyte domain (Fig. 2A,A',B). Interestingly, the strongest *Fgfr1* signal was observed in the floor of the 3V, which harbours the β2 subtype (Fig. 2A'), whilst *Fgfr2* was equally strong in both β2 and β1 tanycyte domains, as well as the transition zone between β1 and α-tanycytes (Fig. 2B; (1)). *Fgfr1* expression was also detected in cells of the Arc, DMN and LHA, with strongest expression in the VMN (Fig. 2A). By contrast, *Fgfr2* riboprobes only weakly stained cells in the Arc, VMN, DMN and LHA, as well as subependymal cells of the M.E. (Fig. 2B and data not shown).

Interestingly, *Fgfr3* expression was absent from the ependymal cell wall altogether, instead being abundant in cells scattered uniformly throughout the hypothalamic parenchyma, reminiscent of glial cell distribution (Fig. 2C), as well as spare cells in

the M.E. We combined *Fgfr3* in situ with immunolabelling for glial/ progenitor cell marker, S-100β, only to find prevalent co-expression of these markers, confirming the glial identity of most *Fgfr3*-expressing cells (Fig. 2C,C'). Glial expression of *Fgfr3* is precedented in the embryonic mouse spinal cord, where Fgfr3 delineates most GFAP+ astrocytes (27). Use of Digoxygenin-labelled *Fgfr4* cRNA probes did not yield a stain in our *in situ* hybridization reactions, consistent with a recent qRT-PCR profiling of NPY-GFP+ sorted arcuate cells (28).

Expression of FGF signalling modulators, mediators and targets overlaps with FGF receptors

A key feature of FGF signalling is the transcriptional activation of its own downstream negative regulators to fine-tune intracellular levels of signalling (9). Exploiting this phenomenon, we investigated the domains of *Spry* family and *Mkp3* expression to ascertain exactly where endogenous FGFR signalling may be occurring in the mediobasal hypothalamus. *In situ* hybridization with *Spry1* riboprobes (Fig. 3A, A') yielded a strong signal in β-tanycytes and cells of the Arc, although expression in VMN, DMN and LHA was also evident. Co-labelling with GFAP antibodies revealed a weak expression in the α-tanycyte domain (Fig. 3A'). By contrast, use of *Spry2* riboprobes (Fig. 3B) showed a more restricted pattern, composed of a weak signal in β tanycytes, and scattered expression in the Arc, LHA and subependymal M.E. *Spry3* ISH reactions produced a weak background signal. *Mkp3* signal was restricted to scant cells in the LHA/ Tuberal nucleus (Fig. 3C).

Another transcriptional target of FGF signalling is the transcription factor *Etv4 (Pea3)* [16-19]. To detect the domain of its expression, we double labelled hypothalamic sections of an *Etv4*-GFP reporter mouse, with anti-GFP as well as anti–GFAP antibodies, and observed a GFP signal in cells of caudal VMN and LHA (caudal to bregma –1.94), but not in tanycytes or GFAP+ parenchymal astrocytes (Fig. 3D,D').

MAP Kinase /ERK signaling pathway is a major transducer of FGFR signalling and is inhibited by Sprouty proteins (9). To detect focal activation of this pathway, we immunolabelled for the phosphorylated form of ERK (pERK) and found a positive signal in parenchymal cells (Fig. 3E), particularly in the Arc, DMN and LHA, but not

VMN. With respect to the ependymal compartment, however, we noticed a rostro-caudal difference in pERK stain, with scarce signal in α and β- tanycytes at bregma -1.70 (Fig. 3E'), contrasting with distinct clusters of pERK-positive β1-tanycytes in more caudal sections, at Bregma -2.06 and beyond, until the third ventricle recedes (Fig. 3F, F').

FGF ligands are expressed in tanycytes in two distinct patterns

The presence of FGFRs (IIIc isoforms) and FGF signalling modulators in the hypothalamus is suggestive of a necessity for cognate ligand/s. To delineate the cohort of putative ligands involved, we performed *in situ* hybridization using *Fgf*-specific cRNA probes and used transgenic reporter mice. Four FGF candidates and two main domains of expression emerged from this screen.

The expression domain of *Fgfs-1* and *-9* overlapped in the 3V wall with a restriction to the α-tanycyte domain (Fig. 4A'-A'',B'-B'). Interestingly, ventricular expression of *Fgf9*, as judged by X-gal staining of Fgf9-lacZ brain, was also confined to rostral sections and absent from caudal bregma co-ordinate -1.82, onwards. Parenchymal staining for these FGFs (Fig. 4A, B; Suppl. Fig. 2A, B) was most intense in the VMN, with sporadic staining of cells in the Arc, DMN and LHA. By contrast, expression of *Fgfs -2* and *-18* encompassed β1- as well as α-tanycytes (Fig. 4C,D; Suppl. Fig. 2C). *Fgf2* expression in the α-tanycyte domain tapered off sharply dorsally, and so is therefore likely confined to the more ventral α2-tanycyte subtype, and ventrally, a weak patchy pattern of expression was seen in β2 tanycytes. Fgf18 expression was determined by activation of the tdTomato-dsred marker upon tamoxifen treatment of Fgf18creERT2::Rosa-tdTomato-dsred mice (3-day tamoxifen pulse; 1-day chase; n=2). A tight cluster of tdTomato-expressing (Tom+) cells was observed spanning β1 and ventral α-tanycyte domains, in addition to scarce Tom+ cells in dorsal parts of the 3V epithelium, well beyond tanycyte domain (not shown). It is noteworthy that the tracing paradigm used here to report Fgf18 expression, would also report descendants of Fgf18-expressing cells. Therefore, scarce Tom+ cells in the dorsal 3V epithelium may reflect dispersion of Fgf18-expressing cells away from a focal

source/site of Fgf18 expression, an interpretation that is consistent with *Fgf18 in situ* hybridization data reported by Robins et al. 2013 (5).

Fgf5 and *Fgf17* cRNA probes yielded a clear signal in the hippocampus (Suppl. Fig. 3) indicative of successful ISH reactions, but none in the hypothalamus. Probes for *Fgfs -7, -8* and *-20* gave a diffuse non-specific signal, not too dissimilar from sense probes, and probes for *Fgfs -16* and *-21* did not produce any staining (not shown).

Restriction of intracellular FGFs to the parenchymal cell compartment

In situ hybridization with cRNA probes for intracellular FGFs (11 to 14) revealed a predominant expression in the hypothalamic parenchyma and subependymal cells in the M.E., but a notable absence from tanycytes themselves. *Fgf12* expression showed the broadest pattern, being present in the DMN, Arc and LHA, most strongly in the VMN (Fig. 4E). *Fgf13* was restricted to sparse cells in the DMN and Arc and rarely in cells of LHA and ventrolateral VMN (Fig. 4F; and data not shown). *Fgf14* was expressed by only a few cells in the most dorsomedial part of the Arcuate (Fig. 4G).

Discussion

Extrinsic modulation of FGF signalling in rodents can elicit dramatic changes in metabolism, body weight and plasma glucose clearance, with the hypothalamus being envisaged as an anchor for these effects. Therapeutic use of FGFs requires a better understanding of the foci and mechanisms by which FGFs operate, and, whether endogenous hypothalamic FGF signaling normally has a role to play in these processes. On face value our results, summarised in Table 1 and Fig. 5, identify beta tanycytes as the primary target and FGF-receptors -1 and 2-IIIc isoforms as the main mediators of exogenous or endogenous canonical FGF signaling within the ependymal wall of the 3V. Moreover FGFR1 and FGFR3 appear as key players in hypothalamic parenchyma but with divergent roles. Our study predicts that FGFs 1, 2, 9 and 18, sourced mainly from tanycytes and cells of the Ventromedial nucleus, are the key FGF ligands in any endogenous effects on ependymal and parenchymal cells. Endogenous FGF signaling is evidenced by

intricate expression of FGF pathway modulator and mediators, such as Sproutys and phosphorylated-ERK. Collectively, our data forms an integrative working model (Fig. 5) for testing the regulatory role of FGFs in critical hypothalamic functions.

Comparison with previous profiling studies of the FGF signaling pathway in hypothalamus

Several surverys and atlases (29-32) have documented the presence of FGFs/ FGFRs in the hypothalamus, but most are either of low resolution, or of embryonic stages prior to formation of tanycytes, or are presented in the saggital plane, which does not show the full cohort of 3V ependymal cells and tanycyte subtypes. Expression of *Fgfr1* and *Fgfr2 by* tanycytes had been noted in coronal sections (Allen Brain Atlas), but their precise cellular domain of expression had not been assessed. Recent studies show that the 3V epithelium is highly compartmentalized (1, 33, 34), and here we took advantage of general GFAP exclusion form the beta tanycyte domain to show that *Fgfrs-1* and *-2* are mostly restricted to this tanycyte subtype. Additionally, co-labelling with S100-β enabled us to show that hypothalamic *Fgfr3* is mostly associated with glial cells. Noteworthy here is the growing importance of hypothalamic glial cells in the modulation of energy balance-regulating neural circuits, through neuroinflammatory processes or otherwise (35). Much less has been known about the domains of FGF signaling modulators and here we highlight Sprys -1 and -2 as putative negative regulators of FGF signalling in tanycytes and hypothalamic neurons, although SPRYs can also operate downstream of other signaling pathways. With respect to FGF ligands, we can not exclude the possibility that other endogenous FGFs, such as 7, 8, 16, 20 and 21, for which are detected by RT-PCR but not in ISH reactions, are also involved in hypothalamic functions. Exogenously-applied FGFs -8 and -17 can certainly improve glucose homoestasis via neurons of the arcuate nucleus (28). Variations across species and/or differential levels of Fgf expression are also possible, as *Fgf5* was detectable by ISH in the rat hypothalamus (36) but not in our study, despite the success of our probes in detecting *Fgf5* in the hippocampus (Suppl. Fig. 3A) in a similar pattern reported by Gomez-Pinilla & Cotman (37). The presence of FGF pathway genes that we have characterized at celllular resolution, is supported by a recent drop-seq gene profiling of cells in the median eminence and the Arcuate nucleus (34). However, it is

possible that with the use of more sensitive methods, such as isotopic *in situ* hybridization or qPCR on cell sorted subpopulations, new and additional members may be identified.

Potential modes and significance of FGF/ FGFR function in tanycytes and parenchymal nuclei

Since canonical FGF signaling requires the activation of FGF-receptors, specifically their IIIc isoforms in hypothalamus (Fig. 1A), FGFRs become the focus of debate when considering FGF function. Activation of FGFRs can yield a multitude of effects, typically involving cell proliferation, differentiation, migration or cytoskeletal remodelling (7). We showed that FGFRs 1 and 2 are restricted to β-tanycytes, where they could regulate cell proliferation and differentation of these newly-identified stem/progenitor cells (38). Indeed, some have envisaged changes in postnatal hypothalamic neurogliogenesis as a contributory mechanism to body-weight change and insulin-independent glucose lowering effects of exogenous FGFs (11, 39). Equally, these effects may involve short or long term alterations in barrier properties, nutrient sensing, and cargoing or trafficking of metabolic signals and hormones by β-tanycytes (2, 38, 40). These cells are certainly enriched in the endocytotic pathway molecules, such as caveolins (41), which have been shown to control FGF2/FGFR1 signalling in other cell types and settings (42). Within the 3V epithelium, β-tanycytes also uniquely possess primary cilia (33), as well as receptors for VEGFR3 (43), and other key regulators of energy homeostasis such as CNTF (44) and Leptin (38). This suggests that β-tanycytes may also be responsive to Hedgehog signalling and/or act as a hub of cell signalling, or that their biology relies on synergy between multiple signalling pathways. Therefore, fine dissection of other signalling pathways in tanycytes is warranted.

Beta 2-tanycytes are radial glial-like cells whose processes span the width of the median eminence. Therefore it is possible that FGFRs -1 and -2 operate not only on their apical surfaces, exposed to ventricular-derived FGFs, but also on their basal surfaces that are in close proximity to the capillary plexus of the outer M.E. where capillary fenestrations would readily allow exposure to circulating FGFs. Hints for the heterogeneity and paracine response of β-tanycytes to endogenous FGFs comes from caudal expression of phospho-ERK in β1 tanycytes, complemented by rostral

expression of *Fgf9* in α-tanycytes (Fig. 4B). The rosto-caudal complimentarity of ligands and receptor is intriguing but highly reminiscent of developmental settings, where mesenchymal and epithelial cells express mutually exclusive cohorts of FGF ligands and receptors, to ensure paracrine and uni-directional FGF signaling (9). In the hypothalamus, FGFs that are secreted into the 3V space may well be distributed by beating cilia of 3V ependymal cells (45) to activate distant receptors. This would be akin to critical asymmetrical distribution of FGF8 and Nodal by beating cilia during establishment of left-right asymmetry in early vertebrate embryos (46). Similarly, strong expression of pERK in the Arcuate (Fig. 3E) and *Etv4-GFP* and *Mkp3* in LH is, complemented by strong expression of *Fgf9* in the neighbouring VMN (Fig. 4B). ERK activation could also reflect receptor activation by FGFs -19 and -21 and Leptin molecules that have crossed the blood-brain barrier. Others studies have suggested that the suprachiasmatic nucleus is the foci of FGF -19/-21 action, since their co-receptor □-klotho is predominantly expressed by this nucleus (32).

The functioning modes of FGF10 and FGFs 12-14 are more engimatic. Within the ependymall wall, Fgf10 expression is also restricted to β-tanycytes (4, 47), but its target receptor, FgfR2-IIIb isoform (10) is absent from the hypothalamus (Fig. 1A). Similarly, FGFs 12-14 do not normally engage FGFRs but are expressed by cells of the hypothalamic parenchyma. Increasing evidence, however, shows that FGFs may also function non-canonically. For example, by trafficking to the nucleus/nucleolus, either alone, or in complex with FGFRs, to induce nuclear cell signaling or to carry out gene-regulating functions via chromatin and RNA-binding properties (48-50). FGFs -13 and -14, respectively, regulate the stabilization of microtubules (51) and proper functioning of voltage-gated sodium and potassium ion channels (52, 53) and so these intracellular FGFs could regulate axonal integrity and transport as well conductivity within neurons of the arcuate (Fig. 4F,G) and other hypothalamic nuclei.

Lessons from human mutations and transgenic mouse models of FGF signaling pathway

Is the prediction of FGFRs 1-3 IIIc and FGFs -1, -2, -9 and -18 as key endogenous canonical FGF signaling partners in mouse hypothalamus, borne out by naturally-occuring human mutations or experimental transgenic alleles? With minor exceptions

(e.g. murine Fgf15 vs human Fgf19), human and mouse FGF signaling apparatus is highly conserved, both in expression domain and function. Moreover, tanycytes have also been identified in the human hypothalamus (54) and human and rodents broadly share common mechanisms for the regulation of energy balance. A spectrum of dominant acting mutations in human FGFRs 1 and 2 cause rare congenital skeletal syndromes, such as Apert and Pfeiffer (55). However, no association between these syndromes and predisposition or resistance to diabetes and obesity has been reported. By contrast, a significant number of achondroplasia patients that carry activating FGFR3 mutations, also manifest atypical obesity (56). Difficulties that bar drawing firm conclusions from human patients though include: the germline nature of these mutations which would additionally impact peripheral organs or indeed multiple brain regions; their rareness, which may preclude statistically valid associations with metabolic/ neuroendocrine defects or diet; and their varied molecular mode of function, with some mutant receptors operating in a FGF ligand-independent manner.

With respect to engineered mouse models, germline deletion of FGFRs -1 and -2, or FGFs -9 or -18 (57) causes prenatal or early postnatal lethality, whilst the loss of FGFR3 induces abnormal bone growth. FGF1 and FGF2-deficient mice, show no overt abnormalities, even as compound mutants. After challenge with high-fat diet, however, these mice show hyperglycemia and insulin resistance, likely due to the critical regulation of adipose tissue by FGF1 (58). Mice carrying a gain-of-Fgfr1 function mutation appear normal (59) but those with a gain-of FgfR2 mutation are hypoglycemic and show growth retardation and early death (60). Fortunately, a plethora of conditional loss and gain of function alleles for these and other FGF/FGFR family genes have been developed to circumvent embryonic/neonatal lethality. Their use in cell-type specific and stage-dependent gene targeting, as exemplified by recent work (28, 61) will prove valuable for unravelling the exact role/s of endogenous FGF signaling, alone or in combination with other signalling pathways, in tanycyte biology and the regulation of hypothalamic neuronal functions.

Figures and Tables

Figure 1. Gross RT-PCR survey of Fibroblast growth factor ligands, receptors, signalling modulators and mediators in the postnatal hypothalamus

RT-PCR products for Fgf-Receptors -1 to -4 (A); *Fgfs* 1-23 (B,B'); and FGF signalling modulators and mediators (C). Underlined numbers and letters denote lack of detection of the relevant genes. Faints bands for *Fgfr2-IIIb* isoform and *Fgf3* are non-specific products, whilst all other RT-PCR products match the expected amplicon size, predicted by use of primers listed in Suppl. Table 1. Multiple *Fgf5* and *Fgf8* products possibly represent isoforms of these genes.

Figure 2. Domain-restricted expression of Fgf-Receptors within the walls of the 3V, and the parenchyma of the mediobasal hypothalamus.

Representative images of *in situ* hybridization experiments using *Fgfr1* (A,A'), *Fgfr2* (B), and *Fgfr3* (C,C') cRNA probes combined with immunohistochemistry for GFAP (A, A') or S100β (C'), and positive control probe, Neuropeptide Y (Npy; D). *Fgfr1* and *Fgfr2* staining in the 3rd ventricle wall is mostly restricted to β-tanycytes (A,A',B). *Fgfr2* expression extends into the transition zone (arrow in B) bordering beta (GFAP$^-$/S100β$^-$) and alpha (GFAP$^+$/S100β$^+$) tanycytes. *Fgfr1* is also expressed in hypothalamic nuclei, outlined by dashed lines (A). (C) Distribution of *Fgfr3* expressing cells in hypothalamic parenchyma (C), with most co-expressing glial cell marker S100β (C', several examples arrowed). (D) *Neuropeptide Y (NpY)* in the rostral part of the arcuate nucleus. Approximate bregma co-ordinates in bottom right corners. Scale bars, 100 μm.

Figure 3. Focal expression of FGF signalling modifiers and mediators. Representative images of *Spry1* (A, A'), *Spry2* (B), *Mkp3* (C) *in situ* hybridization reactions and anti-GFP immunolabelling of *Etv4*-GFP brain sections (D, D'), alone or in combination with GFAP *(*A, A', B, C, D, E, E') or pERK (E, E', F) immunolabelling. *Spry1* is found in β- and α-tanycyte domains as well as hypothalamic parenchyma (A, A'); *Spry2* is observed in β-tanycytes and sporadic cells in hypothalamic

parenchyma (B). *Mkp3* (C; black arrowheads) and *Etv4* (D, D') are both found only in an area corresponding to the Tuberal nucleus. pERK staining is strong in DMN and Arc nuclei. Although sparse in ependymal layer of 3V anteriorly (E, E'; white arrow), foci of pERK signal is evident caudally in β-tanycytes (F,F' bregma -2.06, arrows). Bregma co-ordinates as indicated in right corners; Scale bars, 100 μm.

Figure 4. Distribution of paracrine- and intracrine-acting FGFs in the hypothalamus.

Representative images showing *in situ* hybridization reactions to detect *Fgf1* (A-A"), *Fgf2* (C), and *Fgfs 12-14* (E-G); X-gal stain to detect *Fgf9* in Fgf9-LacZ reporter mice (B-B"); and tomato-dsred immunolabelling to detect *Fgf18* in tamoxifen-treated Fgf18-creERT2::R26-tomatodsred mice (D,D'). Additional immunolabelling or immunohistochemistry for GFAP in a subset of reactions to reveal the approximate domains of beta and alpha tanycytes (A", B, B'', C, D, D'). Note the similarity in the domains of *Fgf -1* and *-9* expression (A-B"), with a restriction to α-tanycyte domain in the ependymal wall (black arrows in A' and B"), prominence in the VMN, contrasting with the absence of *Fgfs -2* and *-18* in the parenchymal compartment (C-D') and their prevalence in both alpha and β1 tanycyte domains, with a weak salt and pepper *Fgf2* expression in β2 domain. Intracellular *Fgfs* 12-14 also predominate in the parenchymal compartment (E-G), with *Fgf12* showing a broader domain of expression (E). Bregma co-ordinates as indicated in right corners; Scale bars, 100 μm.

Figure 5. Schematic of key FGF signalling partners and their putative modes of FGF function in the mediobasal hypothalamus.

Schematic coronal cross section of hypothalamus from approximate bregma -1.82. Square cobbles – cells lining of the 3V, showing approximate positioning of tanycyte subtypes, including a transition zone (Tz) between α and β subtypes, and their radial processes (thin dashed lines). Grey pentagonal boxes - capillary plexus in the outer zone of the Median Eminence (M.E.), contacted by β-tanycytes. Blue shading denotes the domains of FGF-receptor expression within β-tanycytes, hypothalamic

nuclei, scant subependymal cells in the M.E. and in parenchymal glial cells (star-shaped), as putative targets of FGF action. Navy blue denotes overlap between FgfR1 and FgfR2 expression in the floor of the 3V. Orange and brown represent the domains of canonical (FGFs -1, -2, -9 and -18), and non-canonical (FGFs 11-14) expression. Paracrine (orange lines) and autocrine (curved orange lines) effects may involve FGFs -1, -2, -9 and -18, released by tanycytes into the 3V lumen or supplied to parenchymal cells by α-tanycyte terminals, or produced by parenchymal cells themselves. Plasma-derived FGFs could potentially activate FGFRs via distal β-tanycyte processes. FGFs released into lumen of 3V may circulate and have distant functions beyond the mediobasal hypothalamus (dashed arrows). FGFs 12, 13 and 14 would play non-receptor mediated intracrine functions within the cells of the parenchymal nuclei, most prominently in VMN and Arc, and some subependymal M.E. cells.

Table 1. Distribution of key FGF signalling players within different cellular compartments of the mediobasal hypothalamus. Tapered colouring denotes a gradient of intensity of staining (darker ends, higher levels). Single star (*), denotes scattered cells expressing the gene and double stars (**) denote higher levels of expression or tighter clusters of gene-expressing cells.

Supplementary Table 1. Primer pairs used for the RT-PCR screen and to generate cDNA templates for riboprobe synthesis. All primers sequences are 5' to 3'; top rows, forward, and bottom rows reverse primers used. Second column indicates the expected amplicon size following RT-PCR reactions. Note, a subset of the reverse primers were 5'-tagged with T7-RNA polymerase encoding sequences, as described in material and methods section. Star (*) denotes use of these RT-PCR generated T7-Pol tagged amplicons as templates for riboprobe synthesis.

Supplementary Table 2. Primary and secondary antibodies used in this study. Antibodies used for immunodetection of Digoxygenin-labelled riboprobes in *in situ* hybridization reactions; or for detection of cell type-specific markers (GFAP and

S100β), fluorescent reporter markers (GFP, Tomato-dsred) or cell signalling molecules (phosphorylated ERK). Host species, dilution and sources indicated in columns 2 to 4, respectively.

Supplementary Figure 1. Absence of GFAP-immuno-reactivity from the floor of the 3V wall. Immunolabelling of vibratome sections with Rabbit anti-bovine GFAP antibodies (Chemicon Int.) shows the absence of GFAP from ependymal cells of 3V corresponding to β-tanycyte domains, certainly β2-tanycyes, mirroring a pattern seen with the use of Mouse anti-Porcine GFAP antibodies (Merck), shown in Figures 2 and 4, and referenced in Suppl. Table 2. Arrows point to the ventral limit of GFAP signal. Scale bar, 100 μm.

Supplementary Figure 2. Parenchymal distribution and domain-restricted ependymal expression of Fgf1, Fgf9 and Fgf2. High (A, B) and Low (C) power images showing, complementing images shown in Figure 4 A-C, to better depict the parenchymal distribution and domain-restricted ventricular expression (black arrows) of *Fgf1* (A), Fgf9 (B) and *Fgf2* (C), as determined by *in situ* hybridization (A,C) or analysis of a lacZ-reporter (B). Note the absence of *Fgf2* from the parenchymal nuclei. Scale bars, 100 μm.

Supplementary Figure 3. Positive expression of Fgfs -5, -17 and -11 in the hippocampus. Representative images of coronal brain sections subjected to *in situ* hybridization reactions with antisense riboprobes for Fgf5 (A); Fgf17 (B) and Fgf11 (C). Note the positive labelling of the granular layer of the dentate gyrus (DG) and parts of CA1-CA3 fields. Scale bars, 100 μm.

References

1. Goodman T, Hajihosseini MK. Hypothalamic tanycytes-masters and servants of metabolic, neuroendocrine, and neurogenic functions. *Frontiers in neuroscience*. 2015; **9**387.

2. Prevot V, Dehouck B, Sharif A, Ciofi P, Giacobini P, Clasadonte J. The Versatile Tanycyte: A Hypothalamic Integrator of Reproduction and Energy Metabolism. *Endocr Rev*. 2018; **39**(3): 333-68.

3. Lee DA, Bedont JL, Pak T, Wang H, Song J, Miranda-Angulo A, Takiar V, Charubhumi V, Balordi F, Takebayashi H, Aja S, Ford E, Fishell G, Blackshaw S. Tanycytes of the hypothalamic median eminence form a diet-responsive neurogenic niche. *Nat Neurosci*. 2012; **15**(5): 700-2.

4. Haan N, Goodman T, Najdi-Samiei A, Stratford CM, Rice R, El Agha E, Bellusci S, Hajihosseini MK. Fgf10-expressing tanycytes add new neurons to the appetite/energy-balance regulating centers of the postnatal and adult hypothalamus. *J Neurosci*. 2013; **33**6170-80.

5. Robins SC, Stewart I, McNay DE, Taylor V, Giachino C, Goetz M, Ninkovic J, Briancon N, Maratos-Flier E, Flier JS, Kokoeva MV, Placzek M. α-Tanycytes of the adult hypothalamic third ventricle include distinct populations of FGF-responsive neural progenitors. *Nat Commun*. 2013; **4**2049.

6. Ornitz DM, Itoh N. The Fibroblast Growth Factor signaling pathway. *Wiley Interdiscip Rev Dev Biol*. 2015; **4**(3): 215-66.

7. Brewer JR, Mazot P, Soriano P. Genetic insights into the mechanisms of Fgf signaling. *Genes Dev*. 2016; **30**(7): 751-71.

8. Zhang X, Bao L, Yang L, Wu Q, Li S. Roles of intracellular fibroblast growth factors in neural development and functions. *Science China Life Sciences*. 2012; **55**(12): 1038-44.

9. Hajihosseini MK. Fibroblast growth factor signaling in cranial suture development and pathogenesis. *Front Oral Biol*. 2008; **12**160-77.

10. Zhang X, Ibrahimi OA, Olsen SK, Umemori H, Mohammadi M, Ornitz DM. Receptor specificity of the fibroblast growth factor family. The complete mammalian FGF family. *The Journal of biological chemistry*. 2006; **281**15694-700.

11. Gasser E, Moutos CP, Downes M, Evans RM. FGF1 - a new weapon to control type 2 diabetes mellitus. *Nat Rev Endocrinol*. 2017; **13**(10): 599-609.

12. Degirolamo C, Sabba C, Moschetta A. Therapeutic potential of the endocrine fibroblast growth factors FGF19, FGF21 and FGF23. *Nat Rev Drug Discov*. 2016; **15**(1): 51-69.

13. Xu Y, Tamamaki N, Noda T, Kimura K, Itokazu Y, Matsumoto N, Dezawa M, Ide C. Neurogenesis in the ependymal layer of the adult rat 3rd ventricle. *Experimental neurology*. 2005; **192**251-64.

14. Oomura Y, Sasaki K, Suzuki K, Muto T, Li AJ, Ogita Z, Hanai K, Tooyama I, Kimura H, Yanaihara N. A new brain glucosensor and its physiological significance. *The American journal of clinical nutrition*. 1992; **55**278S-82S.

15. Hanai K, Oomura Y, Kai Y, Nishikawa K, Shimizu N, Morita H, Plata-Salaman CR. Central action of acidic fibroblast growth factor in feeding regulation. *Am J Physiol*. 1989; **256**(1 Pt 2): R217-23.

16. Sasaki K, Oomura Y, Li AJ, Hanai K, Tooyama I, Kimura H, Yanaihara N, Hori T. Actions of acidic fibroblast growth factor fragments on food intake in rats. *Obes Res*. 1995; **3 Suppl 5**697S-706S.

17. Sun HD, Malabunga M, Tonra JR, DiRenzo R, Carrick FE, Zheng H, Berthoud H-R, McGuinness OP, Shen J, Bohlen P, Leibel RL, Kussie P. Monoclonal antibody antagonists of hypothalamic FGFR1 cause potent but reversible hypophagia and weight loss in rodents and monkeys. *American journal of physiology Endocrinology and metabolism*. 2007; **292**E964-76.

18. Lelliott CJ, Ahnmark A, Admyre T, Ahlstedt I, Irving L, Keyes F, Patterson L, Mumphrey MB, Bjursell M, Gorman T, Bohlooly-Y M, Buchanan A, Harrison P, Vaughan T, Berthoud H-R, Lindén D. Monoclonal antibody targeting of fibroblast growth factor receptor 1c ameliorates obesity and glucose intolerance via central mechanisms. *PLoS One*. 2014; **9**e112109.

19. Samms RJ, Lewis JE, Lory A, Fowler MJ, Cooper S, Warner A, Emmerson P, Adams AC, Luckett JC, Perkins AC, Wilson D, Barrett P, Tsintzas K, Ebling FJ. Antibody-Mediated Inhibition of the FGFR1c Isoform Induces a Catabolic Lean State in Siberian Hamsters. *Curr Biol*. 2015; **25**(22): 2997-3003.

20. Scarlett JM, Rojas JM, Matsen ME, Kaiyala KJ, Stefanovski D, Bergman RN, Nguyen HT, Dorfman MD, Lantier L, Wasserman DH, Mirzadeh Z, Unterman TG, Morton GJ, Schwartz MW. Central injection of fibroblast growth factor 1 induces sustained remission of diabetic hyperglycemia in rodents. *Nat Med*. 2016; **22**800-6.

21. Huh S-H, Warchol ME, Ornitz DM. Cochlear progenitor number is controlled through mesenchymal FGF receptor signaling. *eLife*. 2015; **4**e05921.

22. Lamballe F, Genestine M, Caruso N, Arce V, Richelme S, Helmbacher F, Maina F. Pool-specific regulation of motor neuron survival by neurotrophic support. *J Neurosci*. 2011; **31**(31): 11144-58.

23. Hajihosseini MK, Heath JK. Expression patterns of fibroblast growth factors-18 and -20 in mouse embryos is suggestive of novel roles in calvarial and limb development. *Mech Dev*. 2002; **113**79-83.

24. Palop JJ, Roberson ED, Cobos I. Step-by-step in situ hybridization method for localizing gene expression changes in the brain. *Methods Mol Biol*. 2011; **670**207-30.

25. Bouret SG. Development of Hypothalamic Circuits That Control Food Intake and Energy Balance. In: nd, Harris RBS, eds. *Appetite and Food Intake: Central Control*. Boca Raton (FL) 2017: 135-54.

26. Hajihosseini MK, Dickson C. A Subset of Fibroblast Growth Factors (Fgfs) Promote Survival, but Fgf-8b Specifically Promotes Astroglial Differentiation of Rat Cortical Precursor Cells. *Molecular and Cellular Neuroscience*. 1999; **14**468-85.

27. Pringle NP, Yu WP, Howell M, Colvin JS, Ornitz DM, Richardson WD. Fgfr3 expression by astrocytes and their precursors: evidence that astrocytes and oligodendrocytes originate in distinct neuroepithelial domains. *Development*. 2003; **130**(1): 93-102.

28. Liu S, Marcelin G, Blouet C, Jeong JH, Jo YH, Schwartz GJ, Chua S, Jr. A gut-brain axis regulating glucose metabolism mediated by bile acids and competitive fibroblast growth factor actions at the hypothalamus. *Mol Metab*. 2018; **8**37-50.

29. Yaylaoglu MB, Titmus A, Visel A, Alvarez-Bolado G, Thaller C, Eichele G. Comprehensive expression atlas of fibroblast growth factors and their receptors generated by a novel robotic in situ hybridization platform. *Dev Dyn*. 2005; **234**371-86.

30. Lein ES, Hawrylycz MJ, Ao N, Ayres M, Bensinger A, Bernard A, Boe AF, Boguski MS, Brockway KS, Byrnes EJ, Chen L, Chen L, Chen TM, Chin MC, Chong J, Crook BE, Czaplinska A, Dang CN, Datta S, Dee NR, Desaki AL, Desta T, Diep E, Dolbeare TA, Donelan MJ, Dong HW, Dougherty JG, Duncan BJ, Ebbert AJ, Eichele G, Estin LK, Faber C, Facer BA, Fields R, Fischer SR, Fliss TP, Frensley C, Gates SN, Glattfelder KJ, Halverson KR, Hart MR, Hohmann JG, Howell MP, Jeung DP, Johnson RA, Karr PT, Kawal R, Kidney JM, Knapik RH, Kuan CL, Lake JH, Laramee AR, Larsen KD, Lau C, Lemon TA, Liang AJ, Liu Y, Luong LT, Michaels J, Morgan JJ, Morgan RJ, Mortrud MT, Mosqueda NF, Ng LL, Ng R, Orta GJ, Overly CC, Pak TH, Parry SE, Pathak SD, Pearson OC, Puchalski RB, Riley ZL, Rockett HR, Rowland SA, Royall JJ, Ruiz MJ, Sarno NR, Schaffnit K, Shapovalova NV, Sivisay T, Slaughterbeck CR, Smith SC, Smith KA, Smith BI, Sodt AJ, Stewart NN, Stumpf KR, Sunkin SM, Sutram M, Tam A, Teemer CD, Thaller C, Thompson CL, Varnam LR, Visel A, Whitlock RM, Wohnoutka PE, Wolkey CK, Wong VY, Wood M, Yaylaoglu MB, Young RC, Youngstrom BL, Yuan XF, Zhang B, Zwingman TA, Jones AR. Genome-wide atlas of gene expression in the adult mouse brain. *Nature*. 2007; **445**(7124): 168-76.

31. Fon Tacer K, Bookout AL, Ding X, Kurosu H, John GB, Wang L, Goetz R, Mohammadi M, Kuro-o M, Mangelsdorf DJ, Kliewer SA. Research resource: Comprehensive expression atlas of the fibroblast growth factor system in adult mouse. *Mol Endocrinol*. 2010; **24**(10): 2050-64.

32. Bookout AL, de Groot MH, Owen BM, Lee S, Gautron L, Lawrence HL, Ding X, Elmquist JK, Takahashi JS, Mangelsdorf DJ, Kliewer SA. FGF21 regulates metabolism and circadian behavior by acting on the nervous system. *Nat Med*. 2013; **19**(9): 1147-52.

33. Mirzadeh Z, Kusne Y, Duran-Moreno M, Cabrales E, Gil-Perotin S, Ortiz C, Chen B, Garcia-Verdugo JM, Sanai N, Alvarez-Buylla A. Bi- and uniciliated ependymal cells define continuous floor-plate-derived tanycytic territories. *Nat Commun*. 2017; **8**13759.

34. Campbell JN, Macosko EZ, Fenselau H, Pers TH, Lyubetskaya A, Tenen D, Goldman M, Verstegen AM, Resch JM, McCarroll SA, Rosen ED, Lowell BB, Tsai LT. A molecular census of arcuate hypothalamus and median eminence cell types. *Nat Neurosci*. 2017; **20**(3): 484-96.

35. Douglass JD, Dorfman MD, Thaler JP. Glia: silent partners in energy homeostasis and obesity pathogenesis. *Diabetologia*. 2017; **60**(2): 226-36.

36. Li AJ, Ozawa K, Tsuboyama H, Imamura T. Distribution of fibroblast growth factor-5 in rat hypothalamus, and its possible role as a regulator of feeding behaviour. *Eur J Neurosci*. 1999; **11**(4): 1362-8.

37. Gomez-Pinilla F, Cotman CW. Distribution of fibroblast growth factor 5 mRNA in the rat brain: an in situ hybridization study. *Brain Res*. 1993; **606**(1): 79-86.

38. Balland E, Dam J, Langlet F, Caron E, Steculorum S, Messina A, Rasika S, Falluel-Morel A, Anouar Y, Dehouck B, Trinquet E, Jockers R, Bouret SG, Prevot V. Hypothalamic tanycytes are an ERK-gated conduit for leptin into the brain. *Cell Metab*. 2014; **19**(2): 293-301.

39. Seeley RJ, Sandoval DA. Targeting the brain as a cure for type 2 diabetes. *Nat Med*. 2016; **22**(7): 709-11.

40. Benford H, Bolborea M, Pollatzek E, Lossow K, Hermans-Borgmeyer I, Liu B, Meyerhof W, Kasparov S, Dale N. A sweet taste receptor-dependent mechanism of glucosensing in hypothalamic tanycytes. *Glia*. 2017; **65**(5): 773-89.

41. Peruzzo B, Pastor FE, Blazquez JL, Amat P, Rodriguez EM. Polarized endocytosis and transcytosis in the hypothalamic tanycytes of the rat. *Cell Tissue Res*. 2004; **317**(2): 147-64.

42. Feng L, Liao WX, Luo Q, Zhang HH, Wang W, Zheng J, Chen DB. Caveolin-1 orchestrates fibroblast growth factor 2 signaling control of angiogenesis in placental artery endothelial cell caveolae. *J Cell Physiol*. 2012; **227**(6): 2480-91.

43. Hou Y, Shin Y-J, Han EJ, Choi J-S, Park J-M, Cha J-H, Choi J-Y, Lee M-Y. Distribution of vascular endothelial growth factor receptor-3/Flt4 mRNA in adult rat central nervous system. *Journal of Chemical Neuroanatomy*. 2011; **42**(1): 56-64.

44. Kokoeva MV, Yin H, Flier JS. Neurogenesis in the hypothalamus of adult mice: potential role in energy balance. *Science*. 2005; **310**(5748): 679-83.

45. Faubel R, Westendorf C, Bodenschatz E, Eichele G. Cilia-based flow network in the brain ventricles. *Science*. 2016; **353**(6295): 176-8.

46. Meyers EN, Martin GR. Differences in left-right axis pathways in mouse and chick: functions of FGF8 and SHH. *Science*. 1999; **285**(5426): 403-6.

47. Hajihosseini MK, De Langhe S, Lana-Elola E, Morrison H, Sparshott N, Kelly R, Sharpe J, Rice D, Bellusci S. Localization and fate of Fgf10-expressing cells in the adult mouse brain implicate Fgf10 in control of neurogenesis. *Mol Cell Neurosci*. 2008; **37**857-68.

48. Mikolajczak M, Goodman T, Hajihosseini MK. Interrogation of a lacrimo-auriculo-dento-digital syndrome protein reveals novel modes of fibroblast growth factor 10 (FGF10) function. *Biochem J*. 2016; **473**(24): 4593-607.

49. Stachowiak MK, Birkaya B, Aletta JM, Narla ST, Benson CA, Decker B, Stachowiak EK. "Nuclear FGF receptor-1 and CREB binding protein: an integrative signaling module". *J Cell Physiol*. 2015; **230**(5): 989-1002.

50. Kostas M, Lampart A, Bober J, Wiedlocha A, Tomala J, Krowarsch D, Otlewski J, Zakrzewska M. Translocation of Exogenous FGF1 and FGF2 Protects the Cell against Apoptosis Independently of Receptor Activation. *J Mol Biol*. 2018; **430**(21): 4087-101.

51. Wu QF, Yang L, Li S, Wang Q, Yuan XB, Gao X, Bao L, Zhang X. Fibroblast growth factor 13 is a microtubule-stabilizing protein regulating neuronal polarization and migration. *Cell*. 2012; **149**(7): 1549-64.

52. Ali SR, Liu Z, Nenov MN, Folorunso O, Singh A, Scala F, Chen H, James TF, Alshammari M, Panova-Elektronova NI, White MA, Zhou J, Laezza F. Functional Modulation of Voltage-Gated Sodium Channels by a FGF14-Based Peptidomimetic. *ACS Chem Neurosci*. 2018; **9**(5): 976-87.

53. Pablo JL, Pitt GS. FGF14 is a regulator of KCNQ2/3 channels. *Proc Natl Acad Sci U S A*. 2017; **114**(1): 154-9.

54. Koopman ACM, Taziaux M, Bakker J. Age-related changes in the morphology of tanycytes in the human female infundibular nucleus/median eminence. *J Neuroendocrinol*. 2017; **29**(5).

55. Ornitz DM, Itoh N. The Fibroblast Growth Factor signaling pathway. *Wiley Interdiscip Rev Dev Biol*. 2015; **4**(3): 215-66.

56. Saint-Laurent C, Garcia S, Sarrazy V, Dumas K, Authier F, Sore S, Tran A, Gual P, Gennero I, Salles JP, Gouze E. Early postnatal soluble FGFR3 therapy prevents the atypical development of obesity in achondroplasia. *PLoS One*. 2018; **13**(4): e0195876.

57. Hung IH, Schoenwolf GC, Lewandoski M, Ornitz DM. A combined series of Fgf9 and Fgf18 mutant alleles identifies unique and redundant roles in skeletal development. *Dev Biol*. 2016; **411**(1): 72-84.

58. Jonker JW, Suh JM, Atkins AR, Ahmadian M, Li P, Whyte J, He M, Juguilon H, Yin YQ, Phillips CT, Yu RT, Olefsky JM, Henry RR, Downes M, Evans RM. A PPARgamma-FGF1 axis is required for adaptive adipose remodelling and metabolic homeostasis. *Nature*. 2012; **485**(7398): 391-4.

59. Hajihosseini MK, Lalioti MD, Arthaud S, Burgar HR, Brown JM, Twigg SR, Wilkie AO, Heath JK. Skeletal development is regulated by fibroblast growth factor receptor 1 signalling dynamics. *Development*. 2004; **131**(2): 325-35.

60. Hajihosseini MK, Wilson S, De Moerlooze L, Dickson C. A splicing switch and gain-of-function mutation in FgfR2-IIIc hemizygotes causes Apert/Pfeiffer-syndrome-like phenotypes. *Proc Natl Acad Sci U S A*. 2001; **98**(7): 3855-60.

61. Lan T, Morgan DA, Rahmouni K, Sonoda J, Fu X, Burgess SC, Holland WL, Kliewer SA, Mangelsdorf DJ. FGF19, FGF21, and an FGFR1/beta-Klotho-Activating Antibody Act on the Nervous System to Regulate Body Weight and Glycemia. *Cell Metab*. 2017; **26**(5): 709-18 e3.

	3rd Ventricle Wall							
	Median Eminence				Parenchymal Nuclei			
Gene	Subependymal	β2 tanycytes	β1 tanycytes	α tanycytes	Arc	VMN	DMN	LHA
Fgfr1					*		**	**
Fgfr2	*				*	*	*	*
Fgfr3	*				**	**	**	**
Spry1								*
Spry2	*				*			*
Mkp3								*
Etv4								*
pERK	*	*	*	*		*		*
Fgf1					*		**	*
Fgf2								
Fgf9					*		*	*
Fgf18								
Fgf12							**	**
Fgf13	*				**	*	**	*
Fgf14					*			

Figure 1

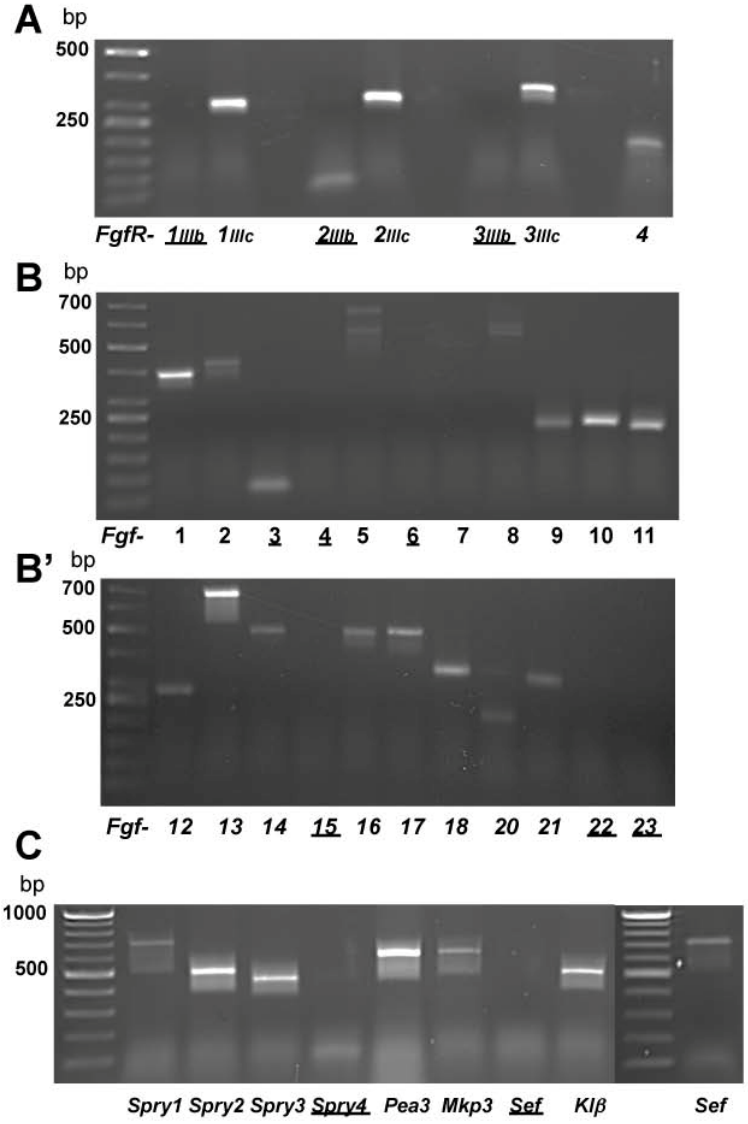

Figure 2

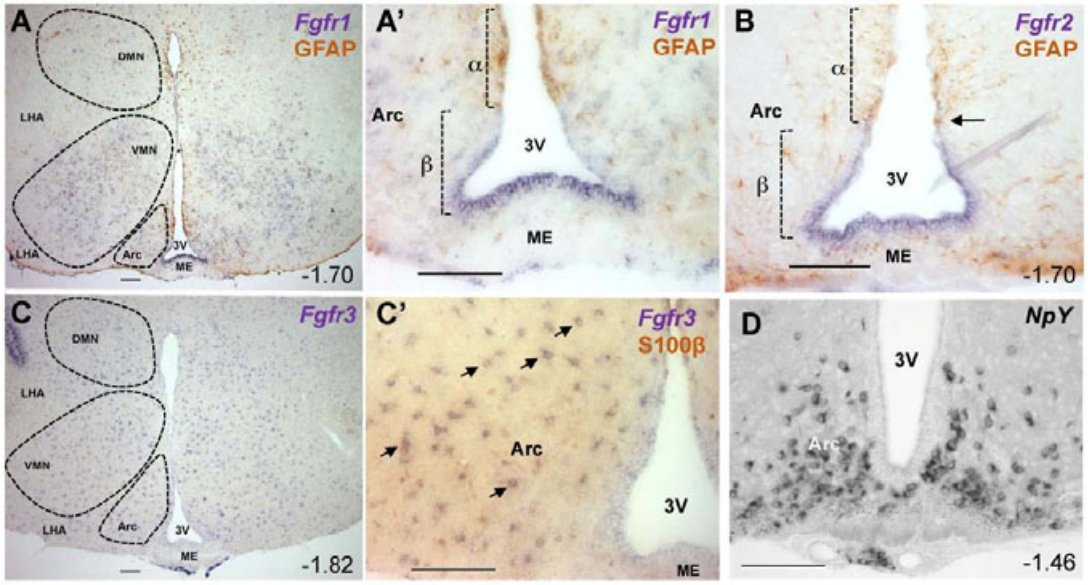

Figure 3

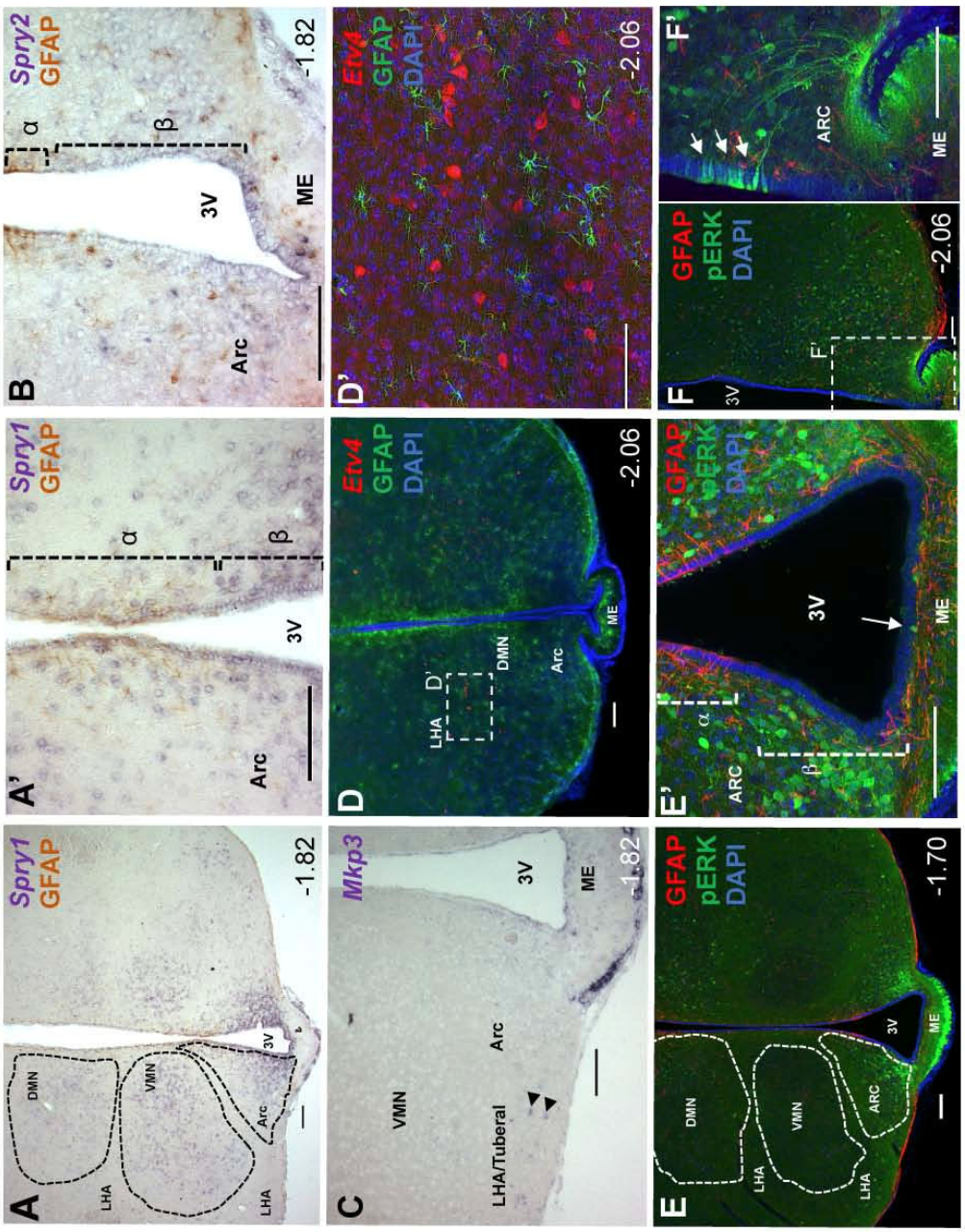

Figure 4

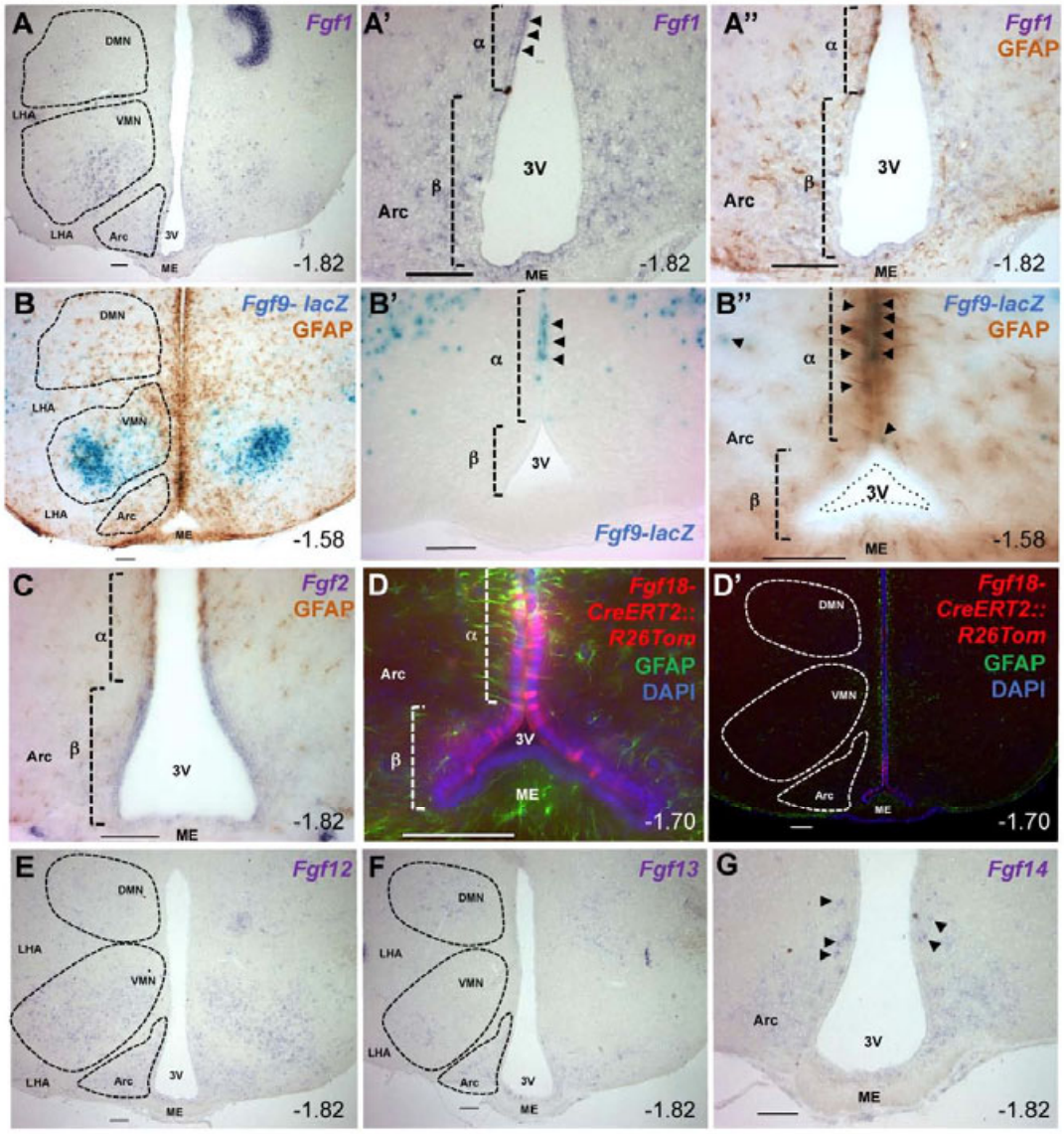

Figure 5